Reactivity Studies of the Zirconium Alkylidene Complexes [η^5-C_5H_3-1,3-($SiMe_2CH_2PPr^i_2$)$_2$]Zr=CHR(Cl) (R = Ph, $SiMe_3$)

Michael D. Fryzuk,*,† Paul B. Duval,† Shane S. S. H. Mao,† Steven J. Rettig,†,‡ Michael J. Zaworotko,§ and Leonard R. MacGillivray§

Contribution from the Departments of Chemistry, University of British Columbia, 2036 Main Mall, Vancouver, BC, Canada V6T 1Z1, and St. Mary's University, Halifax, NS, Canada B3H 3C3

Received July 29, 1998

Abstract: Reactivity studies of the zirconium alkylidene complexes [P_2Cp]Zr=CHR(Cl) (**1a**, R = Ph; **1b**, R = $SiMe_3$; [P_2Cp] = η^5-C_5H_3-1,3-($SiMe_2CH_2PPr^i_2$)$_2$) are described. The reaction of **1** with ethylene follows second-order kinetics to give the ethylene complex [P_2Cp]Zr(η^2-C_2H_4)Cl (**2**), the structure of which was determined by X-ray crystallography. Addition of acetone to **1** generates the alkene RCH=CMe_2, although the anticipated Zr oxo species could not be isolated from this reaction. An insertion of CO into the Zr=C bond of **1** yields the ketene complex [P_2Cp]Zr(η^2-*C,O*-OC=CHR)Cl (**3**), while the reaction with *tert*-butyl isocyanide gives the analogous ketenimine complex [P_2Cp]Zr(η^2-*C,N*-Bu^{t}NC=CHR)Cl (**4**). The structure of ketene **3a** (R = Ph), determined by X-ray diffraction, exhibits the *E* geometry, with the position of the ketene unit with respect to the ancillary [P_2Cp] ligand being opposite to that in the configuration of the precursor alkylidene **1a**. The ketene complex **3** reacts with ethylene to give [P_2Cp]Zr(η^2-*C,O*-CH_2CH_2C(O)=CHR)Cl (**5**). The molecular structure of **5b** (R = $SiMe_3$) was obtained by X-ray diffraction and reveals a five-membered zirconaoxacycle arising from the insertion of ethylene into the Zr−C bond of the ketene, which is subsequently coordinated to the metal as an enolate ligand. **5** undergoes a final insertion reaction with CO to give the asymmetric η^2-acyl−ylide complex **6**. For each reaction detailed above, dissociation of a labile pendant phosphine donor provides an open site for reactivity.

Introduction

Metal alkylidene complexes continue to attract considerable attention by virtue of the diverse reactivity arising from the metal−carbon multiple bond.[1] These species have been utilized as catalysts in a number of transformations involving alkenes[2−5] and alkynes[6] and in stoichiometric Wittig-like olefination reactions with organic carbonyl functionalities.[7−9] Probably the most notable catalytic reaction is the olefin metathesis process[10] for which the ring-opening version[11] has had a huge impact in polymer chemistry, while the ring-closing version[12] is an exciting new synthetic method in organic chemistry.

While alkylidene complexes are especially common for metals from groups 5 and 6, those from group 4 have been limited to a few thermally labile zirconium derivatives[13,14] and a handful of stable Ti examples,[15−19] the majority of which have been generated in situ.[10] In the course of investigating the reactivity of early-metal complexes stabilized by the hybrid donor ancillary ligand η^5-C_5H_3-1,3-($SiMe_2CH_2PPr^i_2$)$_2$ ([P_2Cp]),[20] we reported the isolation of the first thermally stable zirconium alkylidene complexes [P_2Cp]Zr=CHR(Cl) (**1a**, R = Ph; **1b**, R = $SiMe_3$).[21,22] These alkylidene derivatives have been structurally characterized by X-ray crystallography and show a number

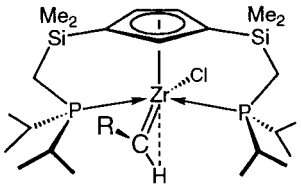

1a R = Ph
1b R = $SiMe_3$

† University of British Columbus.
‡ Professional Officer, UBC X-ray Structural Laboratory.
§ St. Mary's University.

(1) Wilkinson, G.; Stone, F. G. A.; Abel, E. W. *Comprehensive Organometallic Chemistry*, 2nd ed.; Wilkinson, G., Stone, F. G. A., Abel, E. W., Eds.; Pergamon: New York, 1995; Vol. 3.
(2) Wallace, K. C.; Liu, A. H.; Dewan, J. C.; Schrock, R. R. *J. Am. Chem. Soc.* **1988**, *110*, 4964.
(3) Schrock, R. R. *Acc. Chem. Res.* **1990**, *23*, 158.
(4) Herrmann, W. A.; Stumpf, A. W.; Priermeier, T.; Bogdanovic, S.; Dufaud, V.; Basset, J.-M. *Angew. Chem., Int. Ed. Engl.* **1996**, *35*, 2803.
(5) Schuster, M.; Blechert, S. *Angew. Chem., Int. Ed. Engl.* **1997**, *36*, 2036.
(6) Wallace, K. C.; Liu, A. H.; Davis, W. M.; Schrock, R. R. *Organometallics* **1989**, *8*, 644.
(7) Aguero, A.; Kress, J.; Osborn, J. A. *J. Chem. Soc., Chem. Commun.* **1986**, 531.
(8) Schrock, R. R.; dePue, R. T.; Feldman, J.; Schaverien, C. J.; Dewan, J. C.; Liu, A. H. *J. Am. Chem. Soc.* **1988**, *110*, 1423.
(9) Fujimura, O.; Fu, G. C.; Rothemund, P. W. K.; Grubbs, R. H. *J. Am. Chem. Soc.* **1995**, *117*, 2355.
(10) Beckhaus, R. *Angew. Chem., Int. Ed. Engl.* **1997**, *36*, 686.
(11) Schrock, R. R. *Pure Appl. Chem.* **1994**, *66*, 1447.
(12) Grubbs, R. H.; Miller, S. J.; Fu, G. C. *Acc Chem. Res.* **1997**, *28*, 4446.
(13) Schwartz, J.; Gell, K. I. *J. Organomet. Chem.* **1980**, *184*, C1.
(14) Hartner, F. W.; Schwartz, J.; Clift, S. M. *J. Am. Chem. Soc.* **1983**, *105*, 640.
(15) Heijden, H. v. d.; Hessen, B. *J. Chem. Soc., Chem. Commun.* **1995**, 145.
(16) Doorn, J. A. v.; Heijden, H. v. d.; Orpen, A. G. *Organometallics* **1995**, *14*, 1278.
(17) Binger, P.; Muller, P.; Benn, R.; Mynott, R. *Angew. Chem., Int. Ed. Engl.* **1989**, *28*, 610.
(18) Sinnema, P.-J.; Veen, L.; Spek, A. L.; Veldman, N.; Teben, H. H. *Organometallics* **1997**, *16*, 4245.

10.1021/ja982695y CCC: $18.00
Published on Web 02/13/1999

of significant features: An α-agostic C−H interaction orients the alkylidene unit such that the substituent points toward the cyclopentadienyl portion of the ancillary ligand, and the large isopropyl substituents on the coordinated, chelating phosphine donors sterically protect the alkylidene moiety and probably contribute to high thermal stability of these species. Nevertheless, these complexes are reactive, and in this paper, we describe cycloaddition reactions with alkenes, carbon monoxide, and other unsaturated molecules. As these alkylidene complexes are to our knowledge the only stable zirconium derivatives reported to date, an investigation of the their reactivity patterns provides a unique opportunity to examine the results in comparison to the reactivity trends that have been noted for group 5 and 6 alkylidene complexes.

Results and Discussion

Reactivity of [P_2Cp]Zr═CHR(Cl) with Alkenes. As shown in eq 1, the alkylidene complexes [P_2Cp]Zr═CHR(Cl) (**1a**, R = Ph; **1b**, R = $SiMe_3$) react with ethylene as evidenced by the

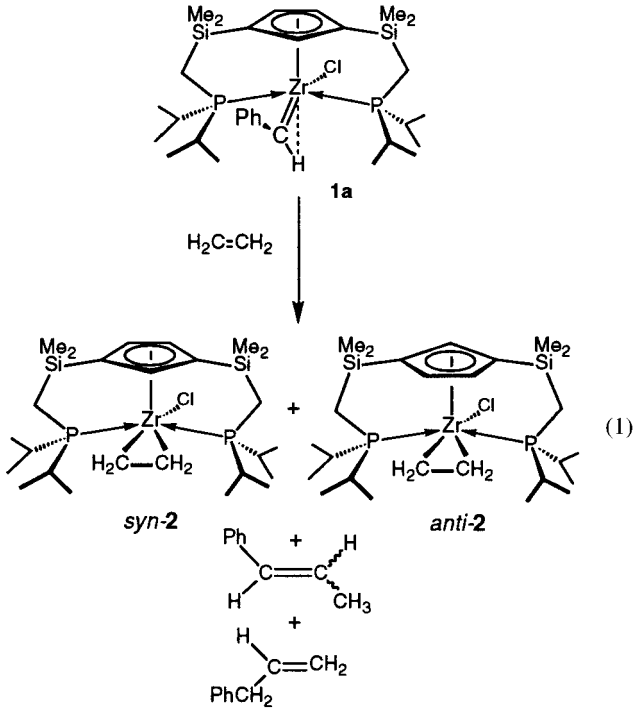

(1)

slow color change from orange to dark red (12 h for **1a**, 8 h for **1b**) to generate two isomeric forms of the ethylene complex [P_2Cp]Zr(η^2-C_2H_4)Cl (**2**) (9:1 ratio). Each isomer of **2** displays a separate singlet in the $^{31}P\{^1H\}$ NMR spectrum and corresponding resonances in the ^1H NMR spectrum, consistent with a structure in which the orientation of the ethylene unit is directed either syn or anti with respect to the unique cyclopentadienyl (Cp) carbon of the ancillary ligand.

The organic byproducts that accompany the conversion of **1** to **2** were detected by ^1H NMR spectroscopy and identified by GC-MS. For example, from benzylidene **1a**, the major product (approximately 70%) is the terminal alkene $PhCH_2CH{=}CH_2$,

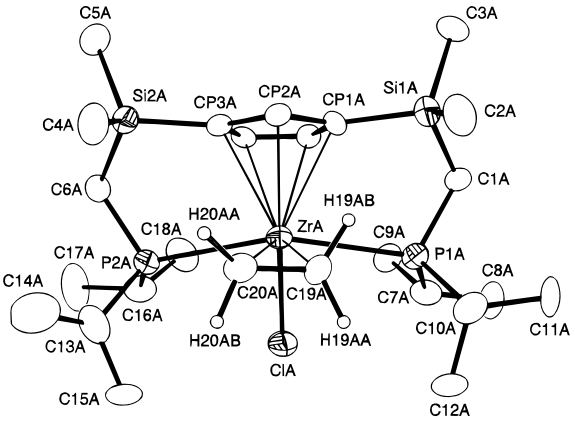

Figure 1. Molecular structure and numbering scheme for [P_2Cp]Zr(η^2-C_2H_4)Cl (**2**).

while the cis and trans isomers of the internal alkene $PhCH{=}CHCH_3$ are obtained in approximately equal quantities. Similar results for **1b** are observed.

In the $^{13}C\{^1H\}$ NMR spectrum of **2** (only peaks due to the major isomer are observed), the ethylene carbon resonances are located upfield at 35 ppm with a $^1J_{CH}$ value of 142 Hz, consistent with hybridization intermediate between sp^2 and sp^3.[23] The ethylene protons give rise to a complex multiplet centered near 1.0 ppm in the ^1H NMR spectrum, originating from an AA′BB′XX′ spin system due to additional $^3J_{PH}$ coupling from the sidearm phosphines. This coupling pattern remains unchanged even at higher temperatures, indicating that the ethylene unit is firmly bound with no evidence for rotation about the metal−ethylene bond axis on the NMR time scale. These spectroscopic data are similar to those of other early-metal ethylene complexes[24−28] and are consistent with a formulation of **2** as a Zr(IV) zirconacyclopropane complex rather than as a Zr(II) adduct. Attempts to determine the stereochemistry (syn or anti) of the major isomer in solution by ^1H NMR spectroscopy by irradiating the Cp proton resonances in an attempt to observe a possible nuclear Overhauser enhancement (nOe) on the protons of the coordinated ethylene fragment were inconclusive.

Some insight into the Zr−ethylene bonding interaction was furnished by a crystal structure determination of *syn*-**2**. The molecular structure is shown in Figure 1, with the crystallographic data given in Table 1 and relevant bond distances and bond angles given in Table 2. The C(19)−C(20) bond distance of 1.439(17) Å is lengthened relative to that of free ethylene (1.337 Å)[29] and is comparable (within 3σ) to that of the only other monomeric Zr−ethylene complex that has been structurally characterized, $Cp_2Zr(\eta^2\text{-}C_2H_4)(PMe_3)$,[30] which has a corresponding C−C bond length of 1.486(8) Å for the ethylene unit. Such elongated C−C bond lengths are indicative of

(19) Kahlert, S.; Görls, H.; Scholz, J. *Angew. Chem., Int. Ed. Engl.* **1998**, *37*, 1857.
(20) Fryzuk, M. D.; Mao, S. S. H.; Duval, P. B.; Rettig, S. J. *Polyhedron* **1995**, *14*, 11.
(21) Fryzuk, M. D.; Mao, S. S. H.; Zaworotko, M. J.; MacGillivray, L. R. *J. Am. Chem. Soc.* **1993**, *115*, 5336.
(22) Fryzuk, M. F.; Duval, P. B.; Mao, S. S. H.; Rettig, S. J.; Zaworotko, M. J.; MacGillivray, L. R. Manuscript in preparation.
(23) Elschenbroich, C.; Salzer, A. *Organometallics*; 2nd ed.; Verlagsgesellschaft: Weinham, Germany, 1992.
(24) McLain, S. J.; Wood, C. D.; Schrock, R. R. *J. Am. Chem. Soc.* **1979**, *101*, 4558.
(25) Takahashi, T.; Murakama, M.; Kunishige, M.; Saburi, M.; Uchida, Y.; Kozawa, K.; Uchida, T.; Swanson, D. R.; Negishi, E. *Chem. Lett.* **1989**, 761.
(26) Takahashi, T.; Suzuki, N.; Kageyama, M.; Nitto, Y.; Saburi, M.; Negishi, E. *Chem. Lett.* **1991**, 1579.
(27) Poole, A. D.; Gibson, V. C.; Clegg, W. *J. Chem. Soc., Chem. Commun.* **1992**, 237.
(28) Thorn, M. G.; Hill, J. E.; Waratuke, S. A.; Johnson, E. S.; Fanwick, P. E.; Rothwell, I. P. *J. Am. Chem. Soc.* **1997**, *119*, 8630.
(29) Bartell, L. S.; Roth, E. A.; Hollowell, C. D.; Kuchitsu, K.; Young, J. E. *J. Chem. Phys.* **1965**, *42*, 2683.
(30) Alt, H. G.; Denner, C. E.; Thewalt, U.; Raush, M. D. *J. Organomet. Chem.* **1988**, *356*, C83.

Table 1. Crystallographic Data

	syn-**2**[a]	*anti*-**3a**[b]	**5b**[c]
formula	$C_{25}H_{51}ClP_2Si_2Zr$	$C_{31}H_{53}ClOP_2Si_2Zr$	$C_{30}H_{61}ClOP_2Si_3Zr$
fw	596.48	686.55	710.69
crystal system	triclinic	monoclinic	monoclinic
space group	$P\bar{1}$ (No. 2)	$P2_1/c$ (No. 14)	$P2_1/c$ (No. 14)
a, Å	15.432(3)	8.666(1)	12.6352(12)
b, Å	20.483(3)	24.244(1)	16.520(2)
c, Å	20.995(7)	17.543(1)	18.5436(4)
α, deg	76.50(3)	90	90
β, deg	83.12(7)	100.936(8)	92.4321(4)
γ, deg	88.52(4)	90	90
V, Å^3	6407(3)	3618.9(6)	3867.1(4)
Z	8	4	4
D_{calc}, g/cm^3	1.24	1.260	1.221
F(000)	2528	1448	1512
μ, cm^{-1}	6.0	5.53	5.49
crystal size, mm	0.30 × 0.40 × 0.45	0.25 × 0.35 × 0.45	0.20 × 0.45 × 0.45
transm factors	0.903−1.00	0.96−1.00	0.57−1.03[d]
scan type	$\omega-2\theta$	$\omega-2\theta$	ω
scan range, deg in ω		0.79 + 0.35 tan θ	0.5
scan speed, deg/min		16 (up to 9 scans)	
data collected	$\pm h,+k,\pm l$	$+h,+k,\pm l$	460 frames, 50 s/f
$2\theta_{max}$, deg	40	60	60
crystal decay, %		2.0	
no. of total reflns	11 928	11 425	36 109[e]
no of. unique reflns	11 917	10 783	9656
R_{merge}	0.023	0.036	0.058
no. of reflns with $I \geq 3\sigma(I)$	7589	5598	5373
no. of variables		344	343
$R(F)$ ($I \geq 3\sigma(I)$)	0.055	0.034	0.056
$R_w(F)$ ($I \geq 3\sigma(I)$)	0.060	0.031	0.053
$R(F^2)$ (all data)	0.055		0.106
$R_w(F^2)$ (all data)	0.060		0.111
gof	3.71	1.49	2.61
max Δ/σ (final cycle)	0.000	0.003	0.007
residual density, e/Å^3	−0.550 to +0.640	−0.35 to +0.31	−2.19 to +1.77 (near Zr)

[a] Temperature 294 K; Nonius CAD-4 diffractometer; Mo Kα radiation (λ = 0.709 30 Å); graphite monochromator; takeoff angle 6.0°; aperture 6.0 × 6.0 mm at a distance of 285 mm from the crystal; stationary-background counts at each end of the scan (scan:background time ratio 2:1); $\sigma^2(F^2) = [S^2(C + 4B)]/(Lp)^2$ (S = scan rate, C = scan count, B = normalized background count); function minimized $\sum w(|F_o| - |F_c|)^2$ where $w = 4F_o^2/\sigma^2(F_o^2)$, $R(F) = \sum||F_o| - |F_c||/\sum|F_o|$, $R_w(F) = [\sum w(|F_o| - |F_c|)^2/\sum w|F_o|^2]^{1/2}$, and gof($F$) = $[\sum w(|F_o| - |F_c|)^2/(m - n)]^{1/2}$. [b] Temperature 294 K; Rigaku AFC6S diffractometer; Mo Kα radiation (λ = 0.710 69 Å); graphite monochromator; takeoff angle 6.0°; aperture 6.0 × 6.0 mm at a distance of 285 mm from the crystal; stationary-background counts at each end of the scan (scan:background time ratio 2:1); $\sigma^2(F^2) = [S^2(C + 4B)]/(Lp)^2$ (S = scan rate, C = scan count, B = normalized background count); function minimized $\sum w(|F_o| - |F_c|)^2$ where $w = 4F_o^2/\sigma^2(F_o^2)$, $R(F) = \sum||F_o| - |F_c||/\sum|F_o|$, $R_w(F) = [\sum w(|F_o| - |F_c|)^2/\sum w|F_o|^2]^{1/2}$, and gof($F$) = $[\sum w(|F_o| - |F_c|)^2/(m - n)]^{1/2}$. [c] Temperature 180 K; Rigaku/ADSC CCD diffractometer; Mo Kα radiation (λ = 0.716 09 Å); graphite monochromator; takeoff angle 6.0°; aperture 94.0 × 94.0 mm at a distance of 39.124(8) mm from the crystal; $\sigma^2(F^2) = (C + B)/(Lp)^2$ (C = scan count, B = background count); function minimized $\sum w(|F_o^2| - |F_c^2|)^2$ where $w = 1/\sigma^2(F_o^2)$, $R(F^2) = \sum||F_o^2| - |F_c^2||/\sum|F_o^2|$, $R_w(F^2) = [\sum w(|F_o^2| - |F_c^2|)^2/\sum w|F_o^2|^2]^{1/2}$, and gof($F^2$) = $[\sum w(|F_o^2| - |F_c^2|)^2/(m - n)]^{1/2}$. Data were collected to $2\theta_{max}$ = 63.7° (full sphere 4−40°, hemisphere 40−60°); all data to $2\theta_{max}$ = 60° were used in the refinement. [d] Includes crystal decay, absorption, and scaling corrections. [e] Includes data to $2\theta_{max}$ = 63.7°.

significant back-bonding from the zirconium and support the metallacyclopropane bonding depiction for **2**. Also consistent with this formalism are the Zr−C bond lengths (average 2.319(11) Å) in *syn*-**2**, which are considerably shorter than the Zr−C distance of 2.68(2) Å in a cationic Zr(IV) olefin complex in which d−π* back-bonding is necessarily absent.[31]

Table 2. Selected Bond Lengths (Å) and Angles (deg) for *syn*-**2**

Zr(1)−Cl(1)	2.500(4)	Zr(1)−P(1)	2.872(4)
Zr(1)−P(2)	2.850(4)	Zr(1)−CP(1)	2.564(11)
Zr(1)−CP(2)	2.605(11)	Zr(1)−CP(3)	2.560(11)
Zr(1)−CP(4)	2.477(11)	Zr(1)−CP(5)	2.47911)
Zr(1)−Cp(4)	2.2361(1)	Zr(1)−Cent(19)	2.2361(16)
Zr(1)−C(20)	2.318(11)	P(1)−C(1)	1.824(12)
P(1)−C(7)	1.865(13)	P(1)−C(10)	1.898(12)
P(2)−C(6)	1.825(12)	P(2)−C(13)	1.886(14)
P(2)−C(16)	1.911(13)	Si(1)−CP(1)	1.858(12)
Si(1)−C(1)	1.877(12)	Si(2)−CP(3)	1.869(12)
Si(2)−C(6)	1.900(13)	CP(1)−CP(2)	1.413(16)
CP(1)−CP(5)	1.431(16)	CP(2)−CP(3)	1.413(16)
CP(3)−C(4)	1.412(16)	CP(4)−CP(5)	1.382(16)
C(19)−C(20)	1.433(17)		

Cl(1)−Zr(1)−P(1)	77.85(12)	Cl(1)−Zr(1)−P(2)	77.42(12)
Cl(1)−Zr(1)−C(19)	98.8(3)	Cl(1)−Zr(1)−C(20)	100.6(3)
P(1)−Zr(1)−P(2)	153.45(11)	P(1)−Zr(1)−C(19)	78.1(3)
P(1)−Zr(1)−C(20)	113.6(3)	P(2)−Zr(1)−C(19)	115.2(3)
P(2)−Zr(1)−C(20)	80.5(3)	C(19)−Zr(1)−C(20)	35.9(4)
Zr(1)−P(1)−C(1)	111.7(4)	Zr(1)−P(2)−C(6)	111.7(4)
CP1(1)−Si(1)−C(1)	102.0(6)	CP(3)−Si(2)−C(6)	102.4(5)
Si(1)−CP(1)−CP(2)	131.1(9)	Si(1)−CP(1)−CP(5)	123.5(9)
P(1)−C(1)−Si(1)	111.6(6)	P(2)−C(6)−Si(2)	112.9(6)

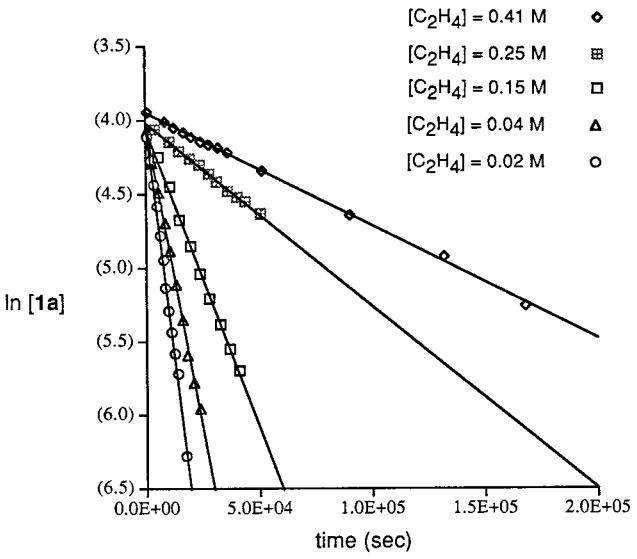

Figure 2. Pseudo-first-order kinetic data for the reaction of [P_2Cp]-Zr=CHPh (**1a**) with ethylene.

Kinetic experiments were conducted to investigate the mechanism of the formation of the ethylene complex **2** from alkylidene **1b**. Figure 2 illustrates a plot of ln [**1b**] vs time for reactions carried out to 2 half-lives for a number of different ethylene concentrations. In all instances, the concentration of ethylene remained essentially unchanged during the course of the reaction, so that the results shown in Figure 2 follow pseudo-first-order behavior consistent with overall second-order kinetics: rate = k[**1a**][C_2H_4].

Although intermediates in the transformation of **1** to **2** were not observed, the second-order kinetics, together with the organic byproducts from reaction 1, are consistent with the reaction mechanism depicted in Scheme 1. The initial coordination of ethylene to **1** is likely assisted by dissociation of one of the potentially labile sidearm phosphines. Subsequent cycloaddition of the coordinated ethylene with the alkylidene moiety gives a

(31) Wu, Z.; Jordan, R. F.; Petersen, J. L. *J. Am. Chem. Soc.* **1995**, *117*, 5867.

Scheme 1

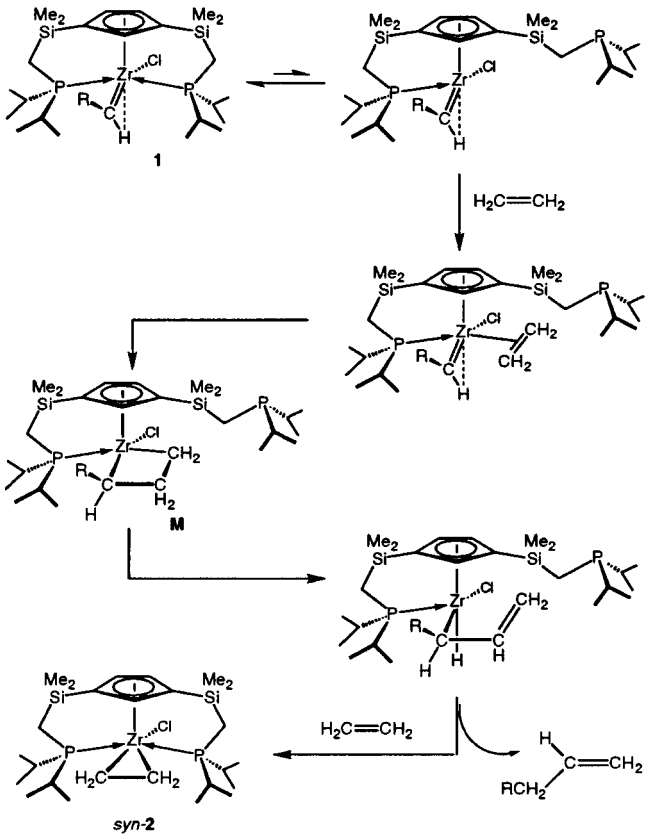

four-membered metallacycle (**M**), an intermediate that has been trapped and isolated[2,16,32] in analogous reactions between alkylidene complexes and certain alkenes. β-Hydride elimination of zirconacyclobutane **M** can occur via two pathways; in Scheme 1, only the pathway that generates the terminal alkene $RCH_2CH{=}CH_2$, the product of the more kinetically favored route, is shown. In the presence of excess ethylene, the zirconium center is trapped by a second equivalent of ethylene, to generate the final product **2**. It is noteworthy that products resulting from alkene metathesis ($RCH{=}CH_2$) were not detected, an indication of the presumed rapid rate for the β-elimination process. This particular mechanism has been generally observed in the reaction of alkylidene complexes with ethylene,[16,18,33] although further coupling from an additional equivalent of ethylene to give a metallacyclopentane[24,34,35] complex has also been noted. However, it was observed that **2** does not react further with additional ethylene. Formation of the anti isomer of **2** could be rationalized by dissociation of the second phosphine, followed by rotation of the cyclopentadienyl group, at some point during the mechanism shown in Scheme 1.

In comparison with some group 5 alkylidene systems,[34] the slow formation of ethylene complex **2** indicates the steric and electronic saturation at the Zr center in alkylidene **1**. When the slightly larger and more weakly binding olefin propene is employed, the reaction is considerably slower, eventually yielding unidentified paramagnetic products after more than 1 week. It is evident that steric crowding from the ancillary [P_2-Cp] ligand restricts the size of molecules that can access the metal center, even with sidearm phosphine dissociation. This point is accentuated by the extremely slow reaction of **1** with the relatively small cumulene allene, to give unidentified products, and the total inability of these alkylidene derivatives to undergo reaction with larger activated substrates such as norbornene, 1,3-butadiene, and internal alkynes.

Reaction of [P_2Cp]Zr=CHR(Cl) with Acetone. Another reaction that is characteristic of early-metal alkylidene complexes is a parallel of the Wittig reaction,[8] and an example is shown in the reaction of **1** with acetone (eq 2). The alkene

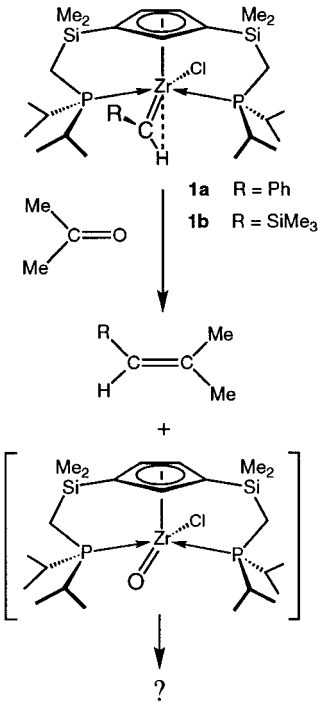

(2)

$RCH{=}C(CH_3)_2$ was isolated and identified by GC-MS, but unfortunately, a Zr-containing species could not be isolated from this reaction. The $^{31}P\{^1H\}$ NMR spectrum of this reaction mixture shows a variety of unidentified species, presumably due to decomposition of the putative oxo species [P_2Cp]ZrO(Cl).

Reaction of [P_2Cp]Zr=CHR(Cl) with CX (X = O, NBu^t). In comparison to the extensive chemistry of alkylidene complexes with alkenes and organic carbonyls, much less attention has been directed toward their reactivity with carbon monoxide and isonitriles. This is somewhat surprising, given that these reactions have been noted to yield unusual ketene and ketenimine complexes,[16,36−38] species that have demonstrated their synthetic utility in a variety of organic transformations.[39−41] Of the ketene complexes obtained by the insertion reaction of metal alkylidenes and CO, structural analysis of the products detailing the mode of insertion have not been reported.

A toluene solution of the alkylidene complex **1** reacts with CO under ambient conditions over a period of 24 h to yield the

(32) Wallace, K. C.; Dewan, J. C.; Schrock, R. R. *Organometallics* **1986**, *5*, 2162.
(33) Fellman, J. D.; Schrock, R. R.; Rupprecht, G. A. *J. Am. Chem. Soc.* **1981**, *103*, 5752.
(34) McLain, S. J.; Wood, C. D.; Schrock, R. R. *J. Am. Chem. Soc.* **1977**, *99*, 3519.
(35) McLain, S. J.; Sancho, J.; Schrock, R. R. *J. Am. Chem. Soc.* **1980**, *102*, 5610.
(36) Cramer, R. E.; Maynard, R. B.; Paw, J. C.; Gilje, J. W. *Organometallics* **1982**, *1*, 869.
(37) Cramer, R. E.; Panchanatheswaran, K.; Gilje, J. W. *J. Am. Chem. Soc.* **1984**, *106*, 1853.
(38) Meinhart, J. D.; Anslyn, E. V.; Grubbs, R. H. *Organometallics* **1989**, *8*, 583.
(39) Sierra, M. A.; Hegedus, L. S. *J. Am. Chem. Soc.* **1989**, *111*, 2335.
(40) Anderson, B. A.; Wulff, W. D.; Rheingold, A. L. *J. Am. Chem. Soc.* **1990**, *112*, 8615.
(41) Brandvold, T. A.; Wulff, W. D.; Rheingold, A. L. *J. Am. Chem. Soc.* **1990**, *112*, 1645.

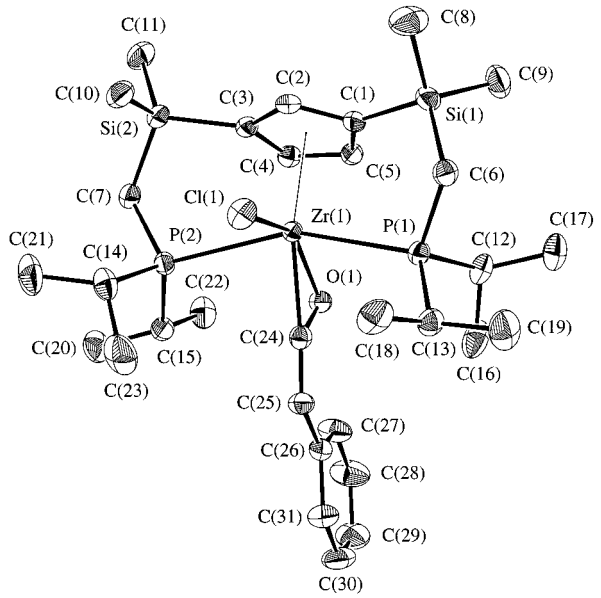

Figure 3. ORTEP view of **3a**, showing 33% probability thermal ellipsoids for the nonhydrogen atoms.

thermally stable ketene complex $[P_2Cp]ZrC(O)=CHR(Cl)$ (**3a**, R = Ph; **3b**, R = $SiMe_3$) in moderate yield (eq 3). Orange

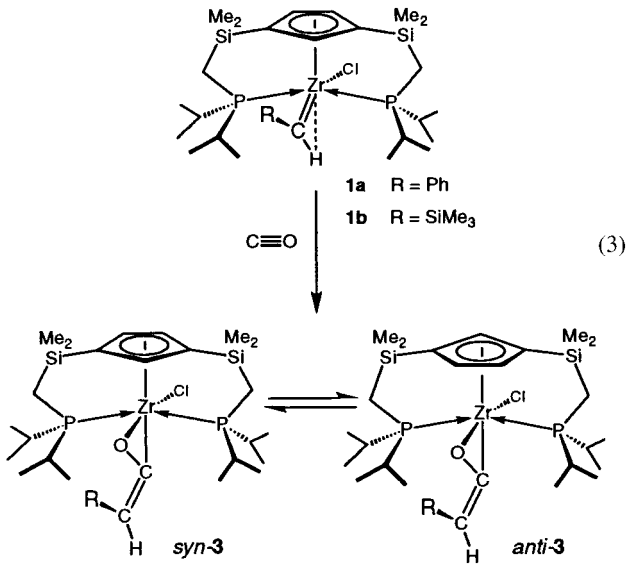

(3)

crystals of **3a** can be isolated from cold hexanes whereas **3b** is obtained as an orange oil which remains soluble in hydrocarbon solvents.

Similar to the solution behavior noted previously for **2**, both **3a** and **3b** exhibit two stereoisomers each, in either a 4:1 (**3a**) or a 2:1 (**3b**) ratio. These species are identified by separate singlets in the $^{31}P\{^1H\}$ NMR spectrum and by corresponding resonances in the ^1H NMR spectrum. Additionally, for each isomer there is a triplet located downfield in the $^{13}C\{^1H\}$ NMR spectrum for the ketene carbon, the observed splitting due to $^2J_{PC}$ coupling to two equivalent phosphines. For **3a**, these resonances are at 192 ppm (minor isomer) and 205 ppm (major isomer), while **3b** exhibits triplets at 203 ppm (major isomer) and 216 ppm (minor isomer), respectively. Again, as with **2**, these stereoisomers are likely the structures *syn*-**3** and *anti*-**3**, which differ in the relative orientation of the ketene unit with respect to the ancillary ligand. It is evident that both species are in equilibrium, as variable-temperature NMR spectroscopy

Table 3. Selected Bond Lengths (Å) and Angles (deg) for *anti*-**3a**[a]

Zr(1)−Cl(1)	2.4976(8)	Zr(1)−P(1)	2.8261(8)
Zr(1)−P(2)	2.8517(8)	Zr(1)−O(1)	2.027(2)
Zr(1)−C(1)	2.572(3)	Zr(1)−C(2)	2.582(3)
Zr(1)−C(3)	2.562(3)	Zr(1)−C(4)	2.523(3)
Zr(1)−C(5)	2.531(3)	Zr(1)−C(24)	2.172(3)
Zr(1)−Cp	2.25	P(1)−C(6)	1.816(3)
P(1)−C(12)	1.851(3)	P(1)−C(13)	1.853(3)
P(2)−C(7)	1.833(3)	P(2)−C(14)	1.849(3)
P(2)−C(15)	1.850(3)	Si(1)−C(1)	1.866(3)
Si(1)−C(6)	1.895(3)	Si(1)−C(8)	1.849(4)
Si(1)−C(9)	1.863(4)	Si(2)−C(3)	1.856(3)
Si(2)−C(7)	1.871(3)	Si(2)−C(10)	1.856(3)
Si(2)−C(11)	1.854(3)	O(1)−C(24)	1.374(3)
C(1)−C(2)	1.416(4)	C(1)−C(5)	1.426(4)
C(2)−C(3)	1.423(4)	C(3)−C(4)	1.427(4)
C(4)−C(5)	1.400(4)	C(24)−C(25)	1.349(4)
C(25)−C(26)	1.465(4)		

Cl(1)−Zr(1)−P(1)	87.66(3)	Cl(1)−Zr(1)−P(2)	86.54(3)
Cl(1)−Zr(1)−O(1)	141.42(6)	Cl(1)−Zr(1)−C(24)	103.43(8)
Cl(1)−Zr(1)−Cp	107.1	P(1)−Zr(1)−P(2)	156.25(2)
P(1)−Zr(1)−O(1)	85.17(5)	P(1)−Zr(1)−C(24)	79.40(7)
P(1)−Zr(1)−Cp	101.9	P(2)−Zr(1)−O(1)	85.10(5)
P(2)−Zr(1)−C(1)	129.25(6)	P(2)−Zr(1)−C(2)	101.95(6)
P(2)−Zr(1)−C(3)	74.84(6)	P(2)−Zr(1)−C(4)	83.77(7)
P(2)−Zr(1)−C(5)	115.64(7)	P(2)−Zr(1)−C(24)	79.60(7)
P(2)−Zr(1)−Cp	101.9	O(1)−Zr(1)−C(1)	116.11(8)
O(1)−Zr(1)−C(2)	138.49(8)	O(1)−Zr(1)−C(3)	118.40(8)
O(1)−Zr(1)−C(4)	88.72(8)	O(1)−Zr(1)−C(5)	87.44(8)
O(1)−Zr(1)−C(24)	37.99(8)	O(1)−Zr(1)−Cp	111.4
C(24)−Zr(1)−Cp	149.4	Zr(1)−P(1)−C(6)	107.12(9)
Zr(1)−P(1)−C(12)	111.42(10)	Zr(1)−P(1)−C(13)	119.25(10)
C(6)−P(1)−C(12)	105.6(1)	C(6)−P(1)−C(13)	106.4(1)
C(12)−P(1)−C(13)	106.2(1)	Zr(1)−P(2)−C(7)	111.01(10)
Zr(1)−P(2)−C(14)	111.7(1)	Zr(1)−P(2)−C(15)	115.04(10)
C(7)−P(2)−C(14)	106.5(1)	C(7)−P(2)−C(15)	104.4(1)
C(14)−P(2)−C(15)	107.6(2)	C(1)−Si(1)−C(6)	107.2(1)
C(1)−Si(1)−C(8)	109.3(1)	C(1)−Si(1)−C(9)	108.9(2)
C(6)−Si(1)−C(8)	107.9(2)	C(6)−Si(1)−C(9)	113.4(1)
C(8)−Si(1)−C(9)	110.0(2)	C(3)−Si(2)−C(7)	104.4(1)
C(3)−Si(2)−C(10)	109.2(1)	C(3)−Si(2)−C(11)	110.6(1)
C(7)−Si(2)−C(10)	111.4(1)	C(7)−Si(2)−C(11)	109.8(1)
C(10)−Si(2)−C(11)	111.2(2)	Zr(1)−O(1)−C(24)	76.7(1)
Si(1)−C(1)−C(2)	124.7(2)	Si(1)−C(1)−C(5)	130.0(2)
C(2)−C(1)−C(5)	105.2(2)	C(1)−C(2)−C(3)	111.6(2)
Si(2)−C(3)−C(2)	126.8(2)	Si(2)−C(3)−C(4)	128.8(2)
C(2)−C(3)−C(4)	104.4(2)	C(3)−C(4)−C(5)	109.9(2)
C(1)−C(5)−C(4)	108.9(2)	P(1)−C(6)−Si(1)	112.4(1)
P(2)−C(7)−Si(2)	111.2(1)	Zr(1)−C(24)−O(1)	65.3(1)
Zr(1)−C(24)−C(25)	169.5(2)	O(1)−C(24)−C(25)	125.2(3)
C(24)−C(25)−C(26)	129.7(3)		

[a] Cp refers to the unweighted centroid of the C(1−5) ring.

reveals a smooth temperature dependence on the relative concentrations, which correlates well to a van't Hoff plot (ln *K* versus 1/*T*). Unfortunately, assignment of the isomeric species as either syn or anti was not possible because the spectroscopic data are unable to distinguish between the two structures in solution. There can be no nuclear Overhauser enhancement (nOe) between the Cp ring protons and protons within the ketene unit because these nuclei are too far apart. Our attempts to introduce an NMR-active nucleus closer to the Cp ring protons by substituting the chloride of **3** with either a fluoride or an alkyl group were unsuccessful, and a heteronuclear nOe experiment conducted on a sample of **3b** containing a ^{13}C-labeled ketene carbon was also inconclusive. The interconversion of the syn and anti isomers of **3** likely occurs via dissociation of both phosphines followed by a 180° rotation of the ancillary ligand around the Zr−Cp centroid axis.

Crystals suitable for X-ray analysis were obtained for ketene **3a**, and the resulting molecular structure is shown in Figure 3. The crystallographic data are shown in Table 1; relevant bond distances and bond angles given in Table 3. The mononuclear

structure arises from the steric bulk of the ancillary ligand, a feature in common with analogous early-metal ketene complexes, where bulky substituents are required to prevent dimerization.[42−46] The η^2-*C,O* coordination of the ketene fragment is also a typical mode of binding to oxophilic metals[44,45,47,48] and is exhibited here by the short Zr−C(24) and Zr−O distances of 2.172(3) and 2.027(2) Å, respectively, and a correspondingly long C−O distance of 1.374(3) Å. These parameters are similar to the analogous bond distances in another monomeric Zr ketene complex, $Cp^*_2Zr(py)(\eta^2$-*C,O*-OC═$CH_2)$,[44] which are 2.181(2), 2.126(1), and 1.338(2) Å, respectively. The C(24)−C(25) distance of 1.349(4) Å is indicative of a double bond, and the coplanarity of the ketene moiety is illustrated by the dihedral angle of 1.9° involving O, C(24), C(25), and C(26). Additionally, the phenyl ring is also nearly coplanar with the ketene fragment with a tilt angle of 8°, an alignment that presumably optimizes delocalization of electron density over the organic fragment and reduces steric interactions with the ancillary ligand.

Two points can be made regarding the solid-state structure of **3a** in comparison to that of the precursor benzylidene **1a**.[21] First, in the solid state, the molecular structure of the ketene complex corresponds to the anti stereoisomer of **3**, a reversal of the orientation noted for **1a** both in solution and in the solid state; presumably, *anti*-**3** is the least soluble isomer of the two ketene species in equilibrium in solution. The second point is that the ketene carbon−carbon double bond has the *E* geometry; in other words, migratory insertion of CO proceeds with retention of stereochemistry about the zirconium−carbon double bond. This geometry arises from the lack of rotation previously noted[21] in the Zr═C bond of the precursor alkylidene. Furthermore, no *E*/*Z* isomerization is observed for the ketene complexes **3**, and this contrasts with the behavior of some other early-metal ketene complexes that have been studied.[47,48]

As an extension of the insertion reaction that produces **3,** the related reaction with isocyanides was investigated. The addition of *tert*-butyl isocyanide to alkylidene **1a** results in the formation of the analogous ketenimine[49−52] complex $[P_2Cp]Zr(\eta^2$-*C,N*-$Bu^tNC{=}CHPh)Cl$ (**4a**; eq 4). To our knowledge this is the first

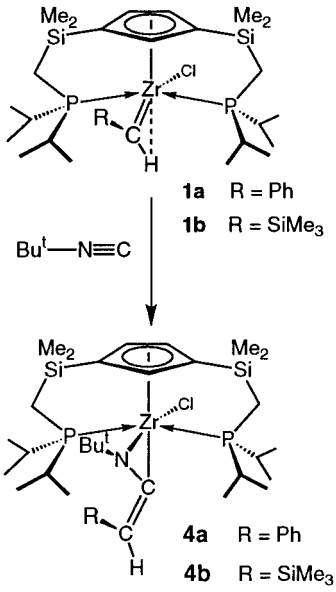

(4)

example of a ketenimine complex obtained from the insertion of an isocyanide into an early-metal alkylidene complex.

Scheme 2

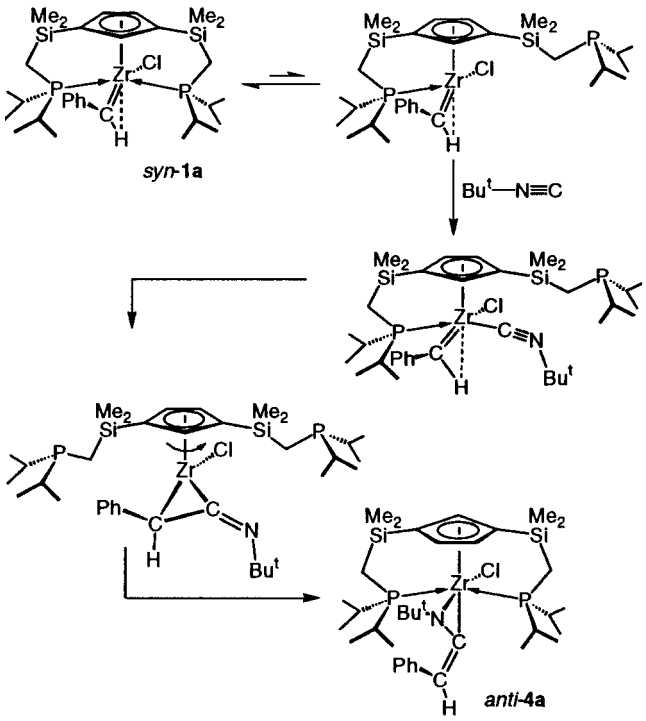

The stoichiometry of this reaction is important because an excess of the isonitrile reacts further with **4** to produce undefined mixtures. Although the spectroscopic parameters for ketenimine **4** are similar to those of the analogous ketene complex, it is interesting to note that, in contrast to the case of **3**, only a single isomer is observed for **4** in solution, presumably because the isomerization process requires rotation of the Cp moiety and this is impeded by the *tert*-butyl group attached to the nitrogen. The steric effects of the large Bu^t group are also apparently manifested in a pronounced broadening of all resonances in the ^{1}H NMR spectrum of protons that are proximate to the *tert*-butyl group of the isocyanide. For **4a**, these include the ortho protons on the phenyl ring and the complete portion of the ancillary ligand that is syn to the ketenimine unit. Of note is the absence of peak broadening for the vinyl proton as the trans geometry situates this proton away from the influence of the *tert*-butyl group, indicating that once again an *E* configuration is adopted despite the apparent steric interaction between the phenyl ring and the *tert*-butyl group. An ^{1}H NOEDIFF NMR experiment conducted on **4** established that the anti isomer is

(42) Meinhart, J. D.; Santarsiero, B. D.; Grubbs, R. H. *J. Am. Chem. Soc.* **1986**, *108*, 3318.

(43) Bristow, G. S.; Hitchcock, P. B.; Lappert, M. F. *J. Chem. Soc., Chem. Commun.* **1982**, 462.

(44) Moore, E. J.; Straus, D. A.; Armantrout, J.; Santarsiero, B. D.; Grubbs, R. H.; Bercaw, J. E. *J. Am. Chem. Soc.* **1983**, *105*, 2068.

(45) Fachinetti, G.; Biran, C.; Floriani, C. *J. Am. Chem. Soc.* **1978**, *100*, 1921.

(46) Scott, M. J.; Lippard, S. J. *J. Am. Chem. Soc.* **1997**, *119*, 3411.

(47) Fermin, M. C.; Hneihen, A. S.; Maas, J. L.; Bruno, J. W. *Organometallics* **1993**, *12*, 1845.

(48) Antiñolo, A.; Otero, A.; Fajardo, M.; López-Mardomingo, C.; Lucas, D.; Mugnier, Y.; Lanfranchi, M.; Pellinghelli, M. *J. Organomet. Chem.* **1992**, *435*, 55.

(49) Antiñolo, A.; Fajardo, M.; López-Mardomingo, C.; Otero, A.; Mourad, Y.; Mugnier, Y.; Aparicio, J.; Fonseca, I.; Florencio, F. *Organometallics* **1990**, *9*, 2919.

(50) Antiñolo, A.; Fajardo, M.; Gil-Sanz, R.; López-Mardomingo, C.; Martín-Villa, P.; Otero, A.; Kubicki, M.; Mugnier, Y.; Krami, S.; Mourad, Y. *Organometallics* **1993**, *12*, 381.

(51) Antiñolo, A.; Fajardo, M.; Gil-Sanz, R.; López-Mardomingo, C.; Otero, A.; Atmani, A.; Kubicki, M.; Krami, S.; Mugnier, Y.; Mourad, Y. *Organometallics* **1994**, *13*, 1200.

(52) Fandos, R.; Lanfranchi, M.; Otero, A.; Pellinghelli, M.; Ruiz, M.; Teuben, J. *Organometallics* **1997**, *16*, 5283.

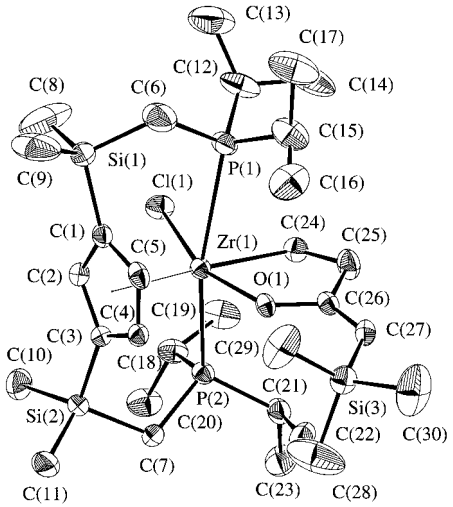

Figure 4. ORTEP view **5b**, showing 50% probability thermal ellipsoids for the nonhydrogen atoms.

obtained, since irradiating the methyl resonance of the *tert*-butyl group leads to an enhancement of the peak assigned to the two equivalent Cp protons, while no effect is observed for the corresponding resonance ascribed to the unique Cp proton. However, if neither the precursor alkylidene **1a** nor the product ketenimine **4a** undergoes syn/anti isomerization, then the transformation from *syn*-**1a** to *anti*-**4a** must occur *during* the migratory insertion of the isocyanide into the Zr−C alkylidene bond (Scheme 2). In this instance, the bulky *tert*-butyl group is directed away from the ancillary ligand until the final step when the nitrogen atom binds to give the η^2-*C,N*-coordinated ketenimine complex. The same mechanism is likely operative in the formation of ketene **3**, although as mentioned previously, this complex is capable of isomerizing after the product is formed.

Further Insertion Reactivity of Ketenes [P$_2$Cp]Zr(η^2-*C,O*-C(O)═CHR)Cl. Addition of ethylene to a toluene solution of ketene **3** results in the slow formation of the insertion product [P$_2$Cp]Zr(η^2-*C,O*-CH$_2$CH$_2$C(O)═CHR)Cl (**5a**, R = Ph; **5b**, R = SiMe$_3$; eq 5).

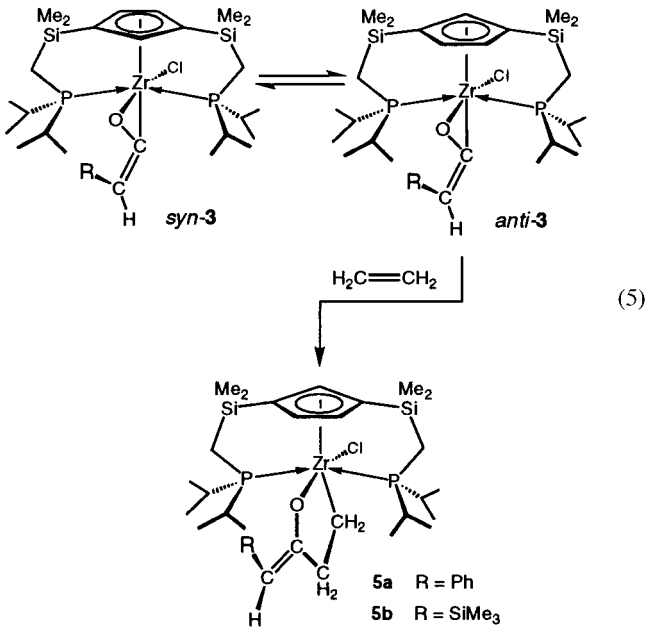

(5)

The ^{1}H and ^{31}P{^{1}H} NMR spectra reveal that both **5a** and **5b** exist as a single species in solution, despite the fact that precursor **3** consists of an equilibrium mixture of two stereoisomers. This suggests either that one isomer of **3** is kinetically more reactive or that both possible stereoisomers of **5** are initially formed, followed by complete conversion of the less stable isomer to the thermodynamically favored observed product.

We were able to isolate crystals of **5b** suitable for an X-ray structure determination; the molecular structure is shown in Figure 4, with the X-ray data tabulated in Table 1 and the bond distances and bond angles given in Table 4. From the molecular structure, it can be seen that one ethylene molecule has inserted into the Zr−C bond of the ketene unit, which is now bound to Zr via the oxygen atom as an enolate fragment, to give a five-membered metallacycle. The overall configuration of **5b** is retained from the precursor ketene complex where the chloride is oriented syn to the unique cyclopentadienyl carbon, C(2). One other structural point is the short C(26)−C(27) distance of 1.329(5) Å.

Table 4. Selected Bond Lengths (Å) and Angles (deg) for **5b**[a]

Zr(1)−Cl(1)	2.5234(10)	Zr(1)−P(1)	2.9527(11)
Zr(1)−P(2)	2.9007(11)	Zr(1)−O(1)	2.036(2)
Zr(1)−C(1)	2.599(3)	Zr(1)−C(2)	2.630(3)
Zr(1)−C(3)	2.635(3)	Zr(1)−C(4)	2.569(3)
Zr(1)−C(5)	2.547(4)	Zr(1)−C(24)	2.332(3)
Zr(1)−Cp	2.30	P(1)−C(6)	1.829(5)
P(1)−C(12)	1.846(4)	P(1)−C(15)	1.908(5)
P(2)−C(7)	1.826(4)	P(2)−C(18)	1.864(4)
P(2)−C(21)	1.857(4)	Si(1)−C(1)	1.844(4)
Si(1)−C(6)	1.877(5)	Si(1)−C(8)	1.828(6)
Si(1)−C(9)	1.836(6)	Si(2)−C(3)	1.850(4)
Si(2)−C(7)	1.882(4)	Si(2)−C(10)	1.850(4)
Si(2)−C(11)	1.845(4)	Si(3)−C(27)	1.833(4)
Si(3)−C(28)	1.852(6)	Si(3)−C(29)	1.833(5)
Si(3)−C(30)	1.856(5)	O(1)−C(26)	1.354(4)
C(1)−C(2)	1.416(5)	C(1)−C(5)	1.430(5)
C(2)−C(3)	1.426(5)	C(3)−C(4)	1.435(5)
C(4)−C(5)	1.382(5)	C(24)−C(25)	1.519(5)
C(25)−C(26)	1.520(5)	C(26)−C(27)	1.329(5)
Cl(1)−Zr(1)−P(1)	81.39(3)	Cl(1)−Zr(1)−P(2)	86.31(3)
Cl(1)−Zr(1)−O(1)	156.64(6)	Cl(1)−Zr(1)−C(24)	82.83(9)
Cl(1)−Zr(1)−Cp	103.0	P(1)−Zr(1)−P(2)	159.21(3)
P(1)−Zr(1)−O(1)	91.28(7)	P(1)−Zr(1)−C(24)	80.87(10)
P(1)−Zr(1)−Cp	99.3	P(2)−Zr(1)−O(1)	93.50(7)
P(2)−Zr(1)−C(24)	81.02(10)	P(2)−Zr(1)−Cp	99.8
O(1)−Zr(1)−C(24)	74.10(10)	O(1)−Zr(1)−Cp	100.1
C(24)−Zr(1)−Cp	174.2	Zr(1)−P(1)−C(6)	110.2(2)
Zr(1)−P(1)−C(12)	114.19(15)	Zr(1)−P(1)−C(15)	117.5(2)
C(6)−P(1)−C(12)	109.5(3)	C(6)−P(1)−C(15)	99.3(3)
C(12)−P(1)−C(15)	105.0(2)	Zr(1)−P(2)−C(7)	111.70(13)
Zr(1)−P(2)−C(18)	110.91(13)	Zr(1)−P(2)−C(21)	117.49(13)
C(7)−P(2)−C(18)	105.5(2)	C(7)−P(2)−C(21)	103.7(2)
C(18)−P(2)−C(21)	106.6(2)	C(1)−Si(1)−C(6)	104.2(2)
C(1)−Si(1)−C(8)	111.1(2)	C(1)−Si(1)−C(9)	109.7(2)
C(6)−Si(1)−C(8)	114.0(3)	C(6)−Si(1)−C(9)	104.1(3)
C(8)−Si(1)−C(9)	113.1(4)	C(3)−Si(2)−C(7)	104.9(2)
C(3)−Si(2)−C(10)	109.9(2)	C(3)−Si(2)−C(11)	109.9(2)
C(7)−Si(2)−C(10)	113.9(2)	C(7)−Si(2)−C(11)	108.6(2)
C(10)−Si(2)−C(11)	109.6(2)	C(27)−Si(3)−C(28)	111.2(2)
C(27)−Si(3)−C(29)	114.2(2)	C(27)−Si(3)−C(30)	108.1(2)
C(28)−Si(3)−C(29)	106.5(3)	C(28)−Si(3)−C(30)	108.5(3)
C(29)−Si(3)−C(30)	108.2(3)	Zr(1)−O(1)−C(26)	128.4(2)
Si(1)−C(1)−C(2)	127.5(3)	Si(1)−C(1)−C(5)	127.4(3)
C(2)−C(1)−C(5)	104.9(3)	C(1)−C(2)−C(3)	111.2(3)
Si(2)−C(3)−C(2)	128.1(3)	Si(2)−C(3)−C(4)	126.7(3)
C(2)−C(3)−C(4)	104.6(3)	C(3)−C(4)−C(5)	109.4(3)
C(1)−C(5)−C(4)	109.8(4)	P(1)−C(6)−Si(1)	114.1(3)
P(2)−C(7)−Si(2)	111.7(2)	Zr(1)−C(24)−C(25)	110.4(2)
C(24)−C(25)−C(26)	112.9(3)	O(1)−C(26)−C(25)	112.1(3)
O(1)−C(26)−C(27)	121.9(3)	C(25)−C(26)−C(27)	126.0(3)
Si(3)−C(27)−C(26)	128.0(3)		

[a] Cp refers to the unweighted centroid of the C(1−5) ring.

The stereochemical preference for either the syn or the anti orientation is a recurring theme for many of the complexes involving the [P_2Cp] ligand; for example, the alkylidene complexes exist exclusively as the syn isomers whereas the ketene insertion complex **5** is found as the anti stereoisomer. Along the way, the ethylene complex **2** and the ketene derivatives **3** are found as mixtures of stereoisomers. Examination of models based on solid-state structures does not provide any hints as to the origins of these capricious preferences since the apparent differences between the two sides of the [P_2Cp] ligand are unremarkable. If the steric differences are almost negligible, then it seems likely that subtle electronic factors are involved in favoring a particular configuration.

The reaction of the ketene complexes **3** with other small molecules was examined; however, except for the reaction noted above with ethylene, ketene **3** was found to be comparatively inert, showing no reactivity with internal alkynes, butadiene, alkylating reagents, or H_2. Monomeric ketene complexes are generally more reactive to substrates such as alkenes,[23,43] alkynes,[53] and H_2[44] than are the corresponding dimeric derivatives.[53] It is presumed that the bulky nature of the ancillary ligand may contribute to this lack of reactivity. In line with this idea, the even more sterically encumbered ketenimine complex **4** undergoes a considerably slower reaction with ethylene (approximately 5 days), and a clean product could not be isolated.

Metallacycle **5** reacts with carbon monoxide to yield an η^2-acyl−ylide complex (**6a**, R = Ph; **6b**, R = $SiMe_3$) in which the metallacycle has expanded to a six-membered ring to accommodate the insertion of CO (eq 6); a single isomer is

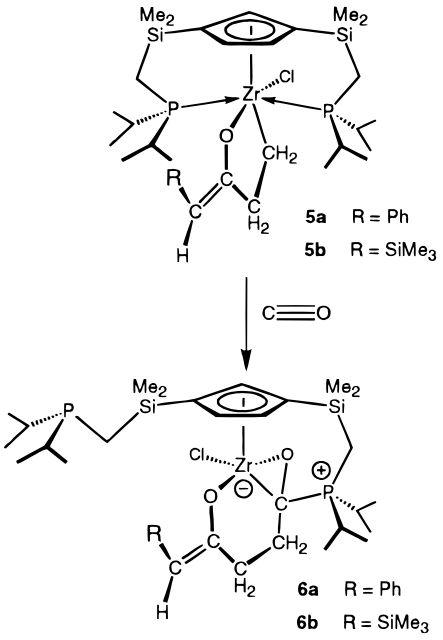

(6)

observed in solution for **6a**, while two species are evident in a 9:1 ratio for **6b**. Particularly diagnostic of such a proposal is the $^{31}P\{^1H\}$ NMR spectrum, in which one observes two singlets, one located downfield near 46 ppm for the ylide phosphine and an upfield peak near 7 ppm corresponding to a free phosphine; the downfield resonance at 46 ppm is very similar to that found for the ylide−formyl complex **7**, for which a resonance at 39.7 ppm was found for the phosphine coordinated to the formyl carbon.[54] The ^1H NMR spectrum of **6a** reveals a complicated second-order splitting pattern for the diastereotopic protons of

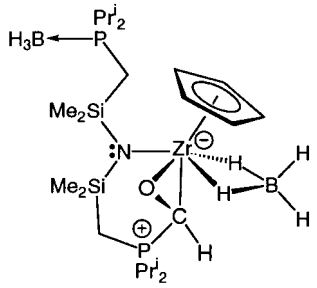

7

the ethylene portion of the metallacycle. For the two protons α to the acyl carbon, this pattern is further complicated by $^3J_{PH}$ coupling, which could be identified by decoupling the phosphorus resonance near 46 ppm. In the acyl−ylide complexes **6**, the newly inserted carbonyl carbon is a chiral center as is the zirconium center. Nevertheless, for **6a**, only one diastereomer is observed, and for **6b**, the observed 9:1 ratio of isomers is likely due to the presence of syn and anti isomers. The low C_1 symmetry of **6** is also evident in the cyclopentadienyl region where three separate resonances are seen in the ^1H NMR spectrum. However, the remainder of the spectrum belies a more symmetric environment, suggesting that the resonances associated with these groups are insensitive to the asymmetry of the molecule.

The sequence of insertion reactions beginning with the alkylidene **1** ceases with the acyl−ylide **6**, which does not react further with CO or with ethylene. The fact that one of the phosphine arms is uncoordinated suggests that the coordination environment around the zirconium center of **6** is effectively saturated, thus preventing any further insertions.

Conclusions

The alkylidene complex **1** undergoes cycloaddition and insertion reactions with a variety of unsaturated substrates. The reactivity at the Zr═C bond is moderated by the sterically bulky [P_2Cp] ancillary ligand, which induces slow reaction rates and imposes a limit on the size of substrates that can access the metal. Although **1** is unreactive with larger olefins and internal alkynes, a reaction of **1** with ethylene follows second-order kinetics to yield the ethylene complex **2** . The solid-state structure of **2** features an elongated C−C bond length for the coordinated ethylene molecule (compared to free ethylene) in agreement with the presence of a zirconacyclopropane unit.

Alkylidene **1** also undergoes migratory insertion reactions with molecules such as CO and CN^tBu to yield η^2-coordinated ketene and ketenimine complexes, **3** and **4**, respectively. Ketene **3** in turn reacts with ethylene to give metallacycle **5**, which undergoes a final insertion of CO to give the η^2-acyl-ylide species **6** (Scheme 3). Such a four-carbon homologation of the original benzylidene fragment is a variant on the alternating copolymerization of CO and ethylene catalyzed by late metal complexes such as those of Pd(II). However, as already noted, for the Zr(IV) system described here, the alternating insertions are stopped at the acyl−ylide stage because the metal center is saturated.

All of the reactions noted above involve an insertion into a Zr−C bond, and a monomeric structure is observed due to the large isopropyl substituents on the pendant phosphines of the ancillary ligand. The potentially labile phosphines likely play

(53) Straus, D. A.; Grubbs, R. H. *J. Am. Chem. Soc.* **1982**, *104*, 5499.

(54) Fryzuk, M. D.; Mylvaganum, M.; Zaworotko, M. J.; MacGillivray, L. R. *Organometallics* **1996**, *15*, 1134.

Scheme 3

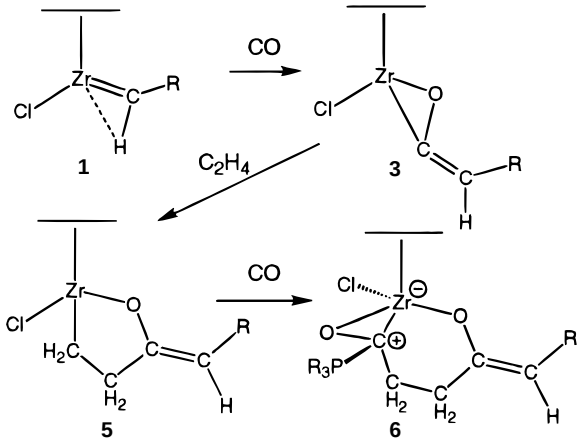

an additional role in providing an open coordination site for these insertion reactions to occur, which accounts for the absence of further insertion chemistry with **6**, where phosphine dissociation to create a reactive site at the metal is not available.

The reactivity of the ethylene complex **2** contrasts with the insertion chemistry presented here and, so, is reported separately in another paper.[55] Related work that is currently in progress is involved with modifying the phosphine substituents from isopropyl to methyl groups to examine the steric effects on the reactivity of alkylidene and related complexes. Preliminary results have indicated that reaction pathways may be altered by this steric modification.

Experimental Section

General Considerations. Unless otherwise stated, all manipulations were performed under an atmosphere of prepurified nitrogen in a Vacuum Atmospheres HE-553-2 glovebox equipped with an MO-40-2H purification system or in standard Schlenk-type glassware on a dual vacuum/nitrogen line. Reactions involving gaseous reagents were conducted in Pyrex vessels (bombs) designed to withstand pressures up to 10 atm. ^{1}H NMR spectra (referenced to either C_6D_5H or $C_6D_5CD_2H$ for benzene or toluene, respectively) were performed on one of the following instruments depending on the complexity of the particular spectrum: Bruker WH-200, Varian XL-300, or Bruker AM-500. ^{13}C NMR spectra (referenced to solvent peaks) were run at 50.323 MHz on the Bruker WH-200 or at 75.429 MHz on the XL-300 instrument, and ^{31}P NMR spectra (referenced to external $P(OMe)_3$ at 141.0 ppm) were run at 121.421 and 202.33 MHz on the XL-300 and Bruker AM-500 instruments, respectively. All chemical shifts are reported in ppm and all coupling constants are reported in Hz. Elemental analyses (Mr. P. Borda) and GC-MS were performed within this department.

Reagents. Ethylene and carbon monoxide were obtained from Matheson and dried over P_2O_5 before use. Labeled ^{13}CO (Cambridge Isotopes) was used as received. *tert*-Butyl isocyanide (Aldrich) was prepared as a toluene solution (0.88 M). Hexanes, tetrahydrofuran (THF), and toluene were predried over CaH_2 followed by distillation under argon from either sodium metal or sodium−benzophenone ketyl; pentane was distilled from sodium−benzophenone ketyl. The deuterated solvents C_6D_6 and $C_6D_5CD_3$ were dried over sodium, vacuum-transferred to a bomb, and degassed by freeze−pump−thaw techniques before use. The procedures for the preparation of [P_2Cp]Zr=CHR(Cl) (**1a**, R = Ph;[21] **5b**, R = $SiMe_3$[22]) have been described elsewhere.

[P_2Cp]Zr(η^2-CH_2=CH_2)Cl (2). Method 1. A solution of **1a** (1.932 g, 2.93 mmol) in 60 mL of toluene was placed in a 200 mL reactor equipped with a needle valve and affixed to a dual vacuum/nitrogen line. A small portion of solvent was removed under vacuum, and an atmosphere of ethylene was introduced at −78 °C. The reaction mixture was warmed to room temperature and left to stir for 12 h, during which the color of the solution gradually changed from bright yellowish-orange to dark red. The solvent was then removed in vacuo, the oily residue was extracted with pentane, and the extract was filtered. Reducing the solution to 7 mL and cooling to −40 °C produced dark red crystals. Yield: 1.61 g (92%).

Method 2. The procedure was identical to that for **1a** above, reacting **1b** with ethylene. A reaction conducted on the same scale as above was complete within 8 h.

^{1}H NMR (20 °C, C_6D_6): δ 0.22 and 0.23 (s, 6H, Si(CH_3)$_2$), 0.78 and 0.83 (d, 2H, $^2J_{PH}$ = 5 Hz, SiCH_2P), 0.99 and 1.04 (m, 2H, ZrCH_2), 1.08, 1.17, 1.22, and 1.29 (dd, 6H, $^3J_{PH}$ = 9 Hz, $^2J_{HH}$ = 7 Hz, CH(CH_3)$_2$), 2.19 (m, 4H, $^2J_{HH}$ = 7 Hz, $^2J_{PH}$ = 7 Hz, CH(CH$_3$)$_2$), 4.32 (t, 1H, $^4J_{HH}$ = 1 Hz, Cp *H*), 6.29 (d, 2H, $^4J_{HH}$ = 1 Hz, Cp *H*). ^{31}P{^{1}H} NMR (20 °C, C_6D_6): δ 19.5 (s). ^{13}C{^{1}H} NMR (20 °C, C_6D_6): δ −2.0 and 1.6 (Si(CH_3)$_2$), 9.3 (SiCH_2P), 9.3, 13.5, 22.7, and 25.4 (CH(CH_3)$_2$), 31.4 (ZrCH_2), 31.5 (CH(CH_3)$_2$), 106.8 (Cp *C*H), 125.9 (Cp *C*H). Anal. Calcd for $C_{25}H_{51}ClP_2Si_2Zr$: C, 50.34; H, 8.62. Found: C, 50.35; H, 8.51.

Kinetic Studies of the Formation of 2. A stock solution was prepared consisting of **1b** (1.75×10^{-2} M) and internal ferrocene standard (6.45×10^{-3} M). For a typical run, a 0.5 mL sample was placed in a 5 mm NMR tube, the solution frozen and degassed, and a partial pressure of ethylene introduced. The tube was then flame-sealed, and ^{1}H NMR spectra were recorded at approximately 40 min intervals for a period of 2−3 half-lives. The concentrations of **5b** and C_2H_4 for each NMR spectrum were measured by peak integration relative to the ferrocene standard; the ethylene concentration remained constant during the reaction period. This procedure was repeated with different ethylene concentrations, to give the plot shown in Figure 2. Similar experiments were conducted at four different temperatures (20, 30, 40, and 50 °C) for the same ethylene concentration to obtain separate reaction rates, which were found to be consistent with second-order kinetics.

[P_2Cp]ZrC(O)=CHPh(Cl) (3a). A solution of **1a** (1.390 g, 2.11 mmol) in 60 mL of toluene was placed in a 200 mL bomb that was affixed to a dual vacuum/nitrogen line. A small portion of solvent was removed under vacuum, and an atmosphere of carbon monoxide was introduced. The reaction mixture was left to stir at room temperature for 48 h, during which the color of the solution gradually changed from bright yellowish-orange to reddish-orange. The solution was then filtered, and the filtrate was reduced to 3 mL and layered with hexanes. Orange crystals were obtained from this solution at −40 °C. Yield: 1.26 g (87%). ^{1}H NMR (20 °C, C_6D_6): δ 0.20 and 0.46 (s, 6H, Si(CH_3)$_2$), 0.70 (dd, 4H, $^2J_{HH}$ = 6 Hz, $^2J_{PH}$ = 7 Hz, SiCH_2P), 0.67, 0.95, 1.20, and 1.36 (dd, 6H, $^3J_{PH}$ = 9 Hz, $^2J_{HH}$ = 7 Hz, CH(CH_3)$_2$), 2.10 (m, 4H, CH(CH$_3$)$_2$), 5.96 (s, 1H, CHPh), 6.60 (d, 2H, $^4J_{HH}$ = 1 Hz, Cp *H*), 7.09 (t, 1H, $^3J_{HH}$ = 7 Hz, C_6H_5 para), 7.14 (t, 1H, $^4J_{HH}$ = 1 Hz, Cp *H*), 7.39 (t, 2H, $^3J_{HH}$ = 7 Hz, C_6H_5 meta), 8.09 (d, 2H, $^3J_{HH}$ = 7 Hz, C_6H_5 ortho). ^{31}P NMR (20 °C, C_6D_6): δ 9.5 (s). ^{13}C NMR (20 °C, C_6D_6): δ −1.4 and 0.7 (Si(CH_3)$_2$), 9.9 (SiCH_2P), 17.5, 19.9, 26.2, and 30.9 (CH(CH_3)$_2$), 102.3 (*C*HPh), 117.1 (CpSi), 122.3 (Cp *C*H$_2$), 125.1 (C_6H_5 para), 126.3 (Cp CH), 129.2 (C_6H_5 meta), 142.0 (C_6H_5 ortho), 205.1 (t, $^2J_{CP}$ = 14 Hz, *C*(O)=C). Anal. Calcd for $C_{31}H_{53}ClOP_2Si_2Zr$: C, 54.23; H, 7.78. Found: C, 54.35; H, 7.85.

[P_2Cp]ZrC(O)=CHSiMe_3(Cl) (3b). The procedure followed was similar to that for **3a**, reacting **1b** (0.98 g, 1.50 mmol) in an atmosphere of CO. The reaction mixture was left to stir at room temperature for 48 h, during which no color change in the solution was noted. The solvent was then removed in vacuo, the oily residue extracted with hexanes, and the extract filtered, yielding a hydrocarbon-soluble orange oil from which crystals could not be obtained. Yield: 0.87 g (85%). Spectroscopic data for the major isomer are as follows. ^{1}H NMR (20 °C, C_6D_6): δ 0.18 and 0.41 (s, 6H, Si(CH_3)$_2$), 0.48 (s, 9H, CHSi(CH_3)$_3$), 0.82 (dd, 4H, $^2J_{HH}$ = 5 Hz, $^2J_{PH}$ = 7 Hz, SiCH_2P), 1.12 (m, 24H, CH(CH_3)$_2$), 2.38 (m, 4H, CH(CH$_3$)$_2$), 4.39 (s, 1H, CHSi(CH$_3$)$_3$), 6.18 (t, 1H, $^4J_{HH}$ = 1 Hz, Cp *H*), 6.43 (d, 2H, $^4J_{HH}$ = 1 Hz, Cp *H*). ^{31}P NMR (20 °C, C_6D_6): δ 11.9 (s).

[P_2Cp]ZrC(N^{t}Bu)=CHPh(Cl) (4a). A toluene solution of 0.088 M *tert*-butyl isocyanide (6.4 mL, 0.56 mmol) was added dropwise with stirring to a cooled (0 °C) solution of **1a** (366 mg, 0.56 mmol) dissolved in 60 mL of toluene. The reaction mixture was stirred at 0 °C for another 30 min and then slowly warmed to room temperature, during which

(55) Fryzuk, M. D.; Duval, P. B.; Rettig, S. J. Manuscript in preparation.

the color of the solution gradually changed from bright orange to dark red. The solution was stirred at room temperature for another 12 h, the solvent then removed in vacuo, the residue extracted with hexanes, and the extract filtered. The solution was reduced to 5 mL, from which dark red crystalline needles were obtained at −40 °C. Yield: 320 mg (77%). ^{1}H NMR (20 °C, C_6D_6): δ 0.20 (br s, 6H, Si(CH_3)$_2$), 0.40 (s, 6H, Si(CH_3)$_2$), 0.69 (m, 4H, SiCH_2P), 1.03 (m, 24H, CH(CH_3)$_2$), 1.57 (s, 9H, N(CH_3)$_3$), 1.82 (m, 2H, CH(CH$_3$)$_2$), 2.49 (br m, 2H, CH(CH$_3$)$_2$), 6.55 (s, 1H, CHPh), 6.80 (d, 2H, $^4J_{HH}$ = 1 Hz, Cp *H*), 6.89 (t, 1H, $^4J_{HH}$ = 1 Hz, Cp *H*), 7.02 (t, 1H, $^3J_{HH}$ = 7 Hz, C_6H_5 para), 7.37 (t, 2H, $^3J_{HH}$ = 7 Hz, C_6H_5 meta), 8.20 (br m, 2H, C_6H_5 ortho). ^{31}P NMR (20 °C, C_6D_6): δ 11.8 (s). IR (C_6D_6): ν_{CN} 1504 cm^{-1}. Anal. Calcd for $C_{35}H_{62}ClNP_2Si_2Zr$: C, 56.68; H, 8.43; N, 1.89. Found: C, 56.85; H, 8.49; N 1.91.

[P$_2$Cp]ZrCH$_2$CH$_2$C(O)═CHPh(Cl) (5a). A solution of **3a** (1.09 g, 1.59 mmol) in 60 mL of toluene was placed in a bomb that was affixed to a dual vacuum line. The headspace was partially evacuated, and an atmosphere of ethylene was introduced. The solution was left to stir at room temperature for 48 h, during which the orange color of the solution slowly turned red. The solvent was then removed in vacuo, the oily residue extracted with hexanes, and the extract filtered. The solution was reduced to 5 mL, from which orange crystals were obtained at −40 °C. Yield: 0.87 g (77%). ^{1}H NMR (20 °C, C_6D_6): δ 0.24 and 0.49 (s, 6H, Si(CH_3)$_2$), 0.72 (dd, 4H, $^2J_{HH}$ = 6 Hz, $^2J_{PH}$ = 7 Hz, SiCH_2P), 0.97 and 1.17 (m, 12H, CH(CH_3)$_2$), 1.50 (m, 2H, ZrCH_2-CH$_2$), 2.09 and 2.21 (m, 2H, CH(CH$_3$)$_2$), 3.41 (t, 2H, $^3J_{HH}$ = 7 Hz, ZrCH$_2$CH_2), 5.43 (s, 1H, CHPh), 6.79 (d, 2H, $^4J_{HH}$ = 2 Hz, Cp *H*), 7.01 (t, 1H, $^4J_{HH}$ = 1 Hz, Cp *H*), 7.06 (t, 1H, $^3J_{HH}$ = 7 Hz, C_6H_5 para), 7.42 (t, 2H, $^3J_{HH}$ = 7 Hz, C_6H_5 meta), 8.05 (d, 2H, $^3J_{HH}$ = 7 Hz, C_6H_5 ortho). ^{31}P NMR (20 °C, C_6D_6): δ 7.8 (s). Anal. Calcd for $C_{33}H_{57}ClOP_2Si_2Zr$: C, 55.47; H, 8.04. Found: C, 55.67; H, 8.19.

[P$_2$Cp]ZrCH$_2$CH$_2$C(O)═CHSiMe$_3$(Cl) (5b). The procedure followed was analogous to that for **5a** above, reacting **3b** (0.80 g, 1.17 mmol) with an atmosphere of ethylene. The reaction mixture was left to stir at room temperature for 36 h, during which there was no change to the orange color of the solution. The solution was concentrated to 2 mL and layered with hexanes, from which orange crystals were obtained at −40 °C from a solution consisting of toluene/hexanes in a 1:1 mixture. Yield: 0.66 g (79%). ^{1}H NMR (20 °C, C_6D_6): δ 0.28 and 0.48 (s, 6H, Si(CH_3)$_2$), 0.47 (s, 18H, CHSi(CH_3)$_3$), 0.91 (d, 4H, $^2J_{HH}$ = 6 Hz, SiCH_2P), 1.11 (m, 24H, CH(CH_3)$_2$), 1.39 (m, 2H, ZrCH_2-CH$_2$), 2.21 (m, 4H, CH(CH$_3$)$_2$), 3.34 (t, 2H, $^3J_{HH}$ = 7 Hz, ZrCH$_2$CH_2), 4.22 (s, 1H, CHSi(CH$_3$)$_3$), 6.59 (d, 2H, $^4J_{HH}$ = 1 Hz, Cp *H*), 6.90 (t, 1H, $^4J_{HH}$ = 1 Hz, Cp *H*). ^{31}P NMR (20 °C, C_6D_6): δ 8.2 (s). Anal. Calcd for $C_{30}H_{61}ClOP_2Si_3Zr$: C, 50.70; H, 8.65. Found: C, 50.60; H, 8.57.

[P$_2$Cp]ZrC(O)CH$_2$CH$_2$C(O)═CHPh(Cl) (6a). A solution of **5a** (0.64 g, 0.90 mmol) in 30 mL of toluene was placed in a bomb that was affixed to a dual vacuum line. An atmosphere of carbon monoxide was introduced at −78 °C, and the reaction mixture was warmed to room temperature and stirred for 24 h, during which the reddish solution gradually faded to an orange-yellow color. The solvent was then reduced to 5 mL and layered with hexanes, from which yellow crystals were obtained at −40 °C. Yield: 0.54 g (80%). ^{1}H NMR (20 °C, C_6D_6): δ 0.01 and 0.28 (s, 6H, Si(CH_3)$_2$), 0.61 (dd, 2H, $^2J_{HH}$ = 6 Hz, $^2J_{PH}$ = 6 Hz, SiCH_2P), 0.71 (dd, 2H, $^2J_{HH}$ = 6 Hz, $^2J_{PH}$ = 6 Hz, SiCH_2P), 0.91 (m, 24H, CH(CH_3)$_2$), 1.62 (m, 4H, CH(CH$_3$)$_2$), 2.19 (m, 2H, C═CCH_2), 2.75 (m, 2H, ZrCCH_2), 5.06 (s, 1H, CHPh), 6.72 (dd, 1H, Cp *H*), 6.83 (dd, 1H, Cp *H*), 7.02 (t, 1H, $^3J_{HH}$ = 7 Hz, C_6H_5 para), 7.23 (dd, 1H, Cp *H*), 7.30 (t, 2H, $^3J_{HH}$ = 7 Hz, C_6H_5 meta), 7.94 (d, 2H, $^3J_{HH}$ = 7 Hz, C_6H_5 ortho),. ^{31}P NMR (20 °C, C_6D_6): δ 46.8 (s), −5.1 (s). Anal. Calcd for $C_{34}H_{57}ClO_2P_2Si_3Zr(C_7H_8)_{0.5}$: C, 57.11; H, 7.80. Found: C, 57.30; H, 7.80.

[P$_2$Cp]ZrC(O)CH$_2$CH$_2$C(O)═CHSiMe$_3$(Cl) (6b). The procedure followed was similar to that for **6a**, reacting **5b** (0.50 g, 0.70 mmol) with an atmosphere of CO. There was no obvious color change to the orange solution after stirring at room temperature for 48 h. The solvent was then removed, the residue extracted with hexanes, and the extract filtered. A yellow-orange crystalline solid was isolated from a cold, concentrated hexanes solution. Yield: 0.39 mg (76%). ^{1}H NMR (20 °C, C_6D_6): δ 0.02, 0.19, 0.32, and 0.49 (s, 3H, Si(CH_3)$_2$), 0.48 (s, 9H, CHSi(CH_3)$_3$), 0.60 (dd, 4H, $^2J_{HH}$ = 7 Hz, $^2J_{PH}$ = 7 Hz, SiCH_2P), 0.85 and 1.09 (m, 12H, CH(CH_3)$_2$), 1.62 (m, 1H, C═CCH_2), 1.67 (m, 4H, CH(CH$_3$)$_2$), 2.04 (dd, 1H, C═CCH_2), 2.21 (dd, 1H, ZrCCH_2), 2.74 (dd, 1H, ZrCCH_2), 4.04 (s, 1H, CHSi(CH$_3$)$_3$), 6.71 (dd, 1H, Cp *H*), 6.83 (dd, 1H, Cp *H*), 7.10 (dd, 1H, Cp *H*). ^{31}P NMR (20 °C, C_6D_6): δ 46.2 (s), −5.9 (s). Anal. Calcd for $C_{31}H_{61}ClO_2P_2Si_3Zr$: C, 50.40; H, 8.32. Found: C, 50.42; H, 8.35.

X-ray Crystallographic Analysis of 2. Diffraction experiments were performed at 23 °C on a Nonius CAD-4 diffractometer equipped with graphite-monochromatized Mo Kα (0.710 69 Å) radiation. The final unit-cell parameters were obtained by least-squares procedures for 24 reflections with 2θ = 30.00−43.00°. The data were processed and corrected for Lorentz and polarization effects and for absorption. The cell parameters were checked with CREDUC for cell reduction, and checks for missing symmetry using MISSYM did not change the space group selected.

The structure was solved by conventional heavy-atom methods, the coordinates of the Zr, P, and Si atoms being determined from the Patterson function and those of the remaining atoms from subsequent difference Fourier syntheses. After anisotropic refinement of all non-hydrogen atoms, methylene and ring sp^2 hydrogen atoms were fixed in calculated positions (d_{C-H} = 1.08 Å), with temperature factors based upon the carbon to which they are bonded. Methyl hydrogen atoms were located and fixed via inspection of a difference Fourier map, with temperature factors based upon the carbon to which they are bonded. H(19) was located via difference Fourier map inspection and refined. All crystallographic calculations were conducted with the PC version of the NRCVAX program package locally implemented on an IBM-compatible 80486 computer.

X-ray Crystallographic Analyses of 3a and 5b. Crystallographic data appear in Table 1. The final unit-cell parameters were obtained by least-squares procedures based on 25 reflections with 2θ = 23.4−32.0° for **3a** and on 27 256 reflections with 2θ = 4.0−63.7° for **5b**. The intensities of three standard reflections, measured every 200 reflections throughout the data collection, decayed linearly by 2.0% for **3a**. The data were processed and corrected for Lorentz and polarization effects, decay (for **3a**), and absorption (empirical, based on azimuthal scans for **3a** and symmetry analysis of redundant data for **5b**).[56,57]

The structures were solved by conventional heavy-atom methods, the coordinates of the heavy atoms being determined from the Patterson functions and those of the remaining atoms from subsequent difference Fourier syntheses. All non-hydrogen atoms were refined with anisotropic thermal parameters. Hydrogen atoms were fixed in idealized positions (C−H = 0.98 Å, $B_H = 1.2B_{\text{bonded atom}}$). A secondary extinction correction was applied for **3a** (Zachariasen type 2 isotropic), the final value of the extinction coefficient being 2.03(4) × 10^{-7}. No correction for secondary extinction was necessary for **5b**. Neutral-atom scattering factors and anomalous dispersion corrections were taken from refs 58 and 59.

Acknowledgment. Financial support for this research was provided by the NSERC of Canada in the form of a Research Grant to M.D.F. and a postgraduate scholarship to P.B.D.

Supporting Information Available: Listings of atomic positional and thermal parameters for **2**, **3a**, and **5b**. This material is available free of charge on the Internet at http://pubs.acs.org.

JA982695Y

(56) *teXsan: Crystal Structure Analysis Package*; Molecular Structure Corp.: The Woodlands, TX, 1985 and 1992.

(57) *d*TREK: Area Detector Software*; Molecular Structure Corp.: The Woodlands, TX, 1997.

(58) *International Tables for X-ray Crystallography*; Kynoch Press: Birmingham, U.K. (present distributor Kluwer Academic Publishers: Boston, MA), 1974; Vol. IV.

(59) *International Tables for Crystallography*; Kluwer Academic Publishers: Boston, MA, 1992; Vol. C.